Colloid Polym Sci (2014) 292:2111–2122
DOI 10.1007/s00396-014-3244-6

ORIGINAL CONTRIBUTION

# Biomimetic star-shaped porphyrin-cored poly(L-lactide)-b-glycopolymer block copolymers for targeted photodynamic therapy

**Xiao-Hui Dai · Zhi-Ming Wang · Wei Liu · Chang-Ming Dong · Jian-Ming Pan · Si-Song Yuan · Yong-sheng Yan · Dong-Ming Liu · Lin Sun**

Received: 23 February 2014 / Revised: 19 April 2014 / Accepted: 24 April 2014 / Published online: 7 May 2014


**Abstract** Porphyrin-cored poly(L-lactide) (SPPLA) was successfully synthesized from ring-opening polymerization (ROP) of L-lactide initiated with porphyrin core. Then, SPPLA was coupled with benzylsulfanylthiocarbonylsufanylpropionic acid (BSPA), and a macro-reversible addition-fragmentation chain transfer (macroRAFT) polymerization agent SPPLA-BSPA was obtained. Finally, star-shaped porphyrin-cored poly(L-lactide)-b-poly(gluconamidoethyl methacrylate) (SPPLA-b-PGAMA) block copolymers were synthesized via RAFT of unprotected gluconamidoethyl methacrylate (GAMA) in 1-methyl-2-pyrrolidinone (NMP) solution at 70 °C. The structure of this block copolymer was thoroughly studied by nuclear magnetic resonance spectroscopy (NMR), gel permeation chromatography (GPC), and differential scanning calorimetry (DSC). Under the irradiation, such SPPLA-b-PGAMA copolymer exhibits efficient singlet oxygen generation and indicates high fluorescence quantum yields. Notably, with UV–vis and dynamic light scattering (DLS) analysis, SPPLA-b-PGAMA showed a very specific recognition with concanavalin A (ConA). Particularly, MTT shows that the cytotoxicity of SPPLA-b-PGAMA against COS-7 cells was very low and, when given a longer irradiation time, more BEL-7402 cancer cells died, which will be investigated in this study.

**Keywords** Glycopolymer · RAFT · Self-assembly · Targeted · Biomolecule recognition

**Electronic supplementary material** The online version of this article (doi:10.1007/s00396-014-3244-6) contains supplementary material, which is available to authorized users.

Mr. Pan has done a prominent work in the study of singlet oxygen research and Fluorescence quantum yield.

X.-H. Dai (✉) · Z.-M. Wang · J.-M. Pan · S.-S. Yuan · Y.-s. Yan
Department of Chemical Engineering, School of Chemistry and Chemical Technology, Jiangsu University, Zhenjiang 212013, People's Republic of China
e-mail: daixiaohui@ujs.edu.cn

X.-H. Dai · Y.-s. Yan
State Key Laboratory of Natural and Biomimetic Drugs, Peking University, Beijing 100191, People's Republic of China

W. Liu · C.-M. Dong
Department of Polymer Science and Engineering, School of Chemistry and Chemical Technology, Shanghai Jiao Tong University, Shanghai 200240, People's Republic of China

D.-M. Liu
Hospital Affiliated to Jiangsu University, Zhenjiang 212013, People's Republic of China

L. Sun
CSR Qingdao Sifang Co. Ltd., Qingdao, Shandong 266111, China

## Introduction

During the last decades, porphyrin used for photodynamic therapy (PDT) is a burgeoning technology for cancer therapy [1, 2]. Porphyrin, as one of the photosensitizers (PSs), when exposed to light of appropriate wavelength, will produce highly reactive oxygen species (ROS) that induce an effective and selective destruction of diseased tissues without damage to the surrounding normal tissues [3, 4]. However, drawbacks such as molecular complexity, self-quenching, photo-toxicity to the skin induced by existing agent' hydrophobicity, and non-selectivity greatly limit its in vivo application [5]. In recent years, reports on star-shaped amphiphilic polymers used for delivering porphyrin have been increasingly studied because the amphiphilic polymer shell could inhibit self-quenching of the porphyrin core [6]. Meanwhile, star-shaped amphiphilic polymers have many other advantages such as flexible architecture, controllable surface functionality, high surface reactivity, and low hydrodynamic radius [7–9].

However, studies on star-shaped amphiphilic porphyrin-cored polymers are still limited since their propensity is to complex and the synthesis process is difficult [10–15]. Frechet [16], Lai [17], and our group [18, 19] have successfully synthesized a series of porphyrin-cored poly(L-lactide)/poly(caprolactone) (PLA/PCL) polymeric shell based on ring-opening polymerization (ROP), but these porphyrin-cored PLA/PCL polymers lack water solubility which significantly limits their further application. Therefore, improving the physical and biodegradation properties of porphyrin-cored PLA/PCL polymer remains an urgent task.

To date, studies focusing on the synthesis of controllable molecular weight and well-defined architecture of glycopolymers have been increased [20–24]. Glycopolymers are synthetic polymers possessing a non-carbohydrate backbone but carrying carbohydrate moieties as pendant or terminal groups and have been used to elucidate the specific sugar–protein recognition processes in living cells, which could be used for drug discovery and biomaterials applications [21, 23, 25–27]. Glycosylation tends to specifically interact with lectin-type receptors overexpressed in the malignant tissue [28–30]. In these work, it is very useful to use the glycopolymers with porphyrin core as recognition motifs and contribute to targeting photosensitizers towards tumor cells. Moreover, it is known that naturally oligosaccharides/polysaccharides often play an important role in stabilizing the molecular structure of protein and can significantly improve the compatibility between hydrophobic polymers and hydrophilic peptide drugs [31, 32].

In this study, novel and well-defined star-shaped porphyrin-cored poly(L-lactide)-b-poly(gluconamidoethyl methacrylate) (SPPLA-b-PGAMA) block copolymers was successfully prepared, as shown in Scheme 1. The molecular structures, self-assembled behavior, fluorescence quantum yield, single oxygen production, and recognition properties of these porphyrin-cored star-shaped SPPLA-b-PGAMA block copolymers were thoroughly characterized. Moreover, the cell viability of this porphyrin-cored glycopolymer, both including cytotoxicity and photo-toxicity, was evaluated. Consequently, this will not only provide potentially porphyrin-cored star-shaped SPPLA-b-PGAMA block copolymers for targeted photodynamic therapy but also improve the physical, biodegradation, and biocompatibility properties of PLA-based biomaterials.

## Experimental section

### Materials

4-Dimethylamiopryidine (DMAP), dicyclohexylcarbodiimide (DCC), 1,6-diphenyl-1,3,5-hexatriene (DPH), and concanavalin A (ConA) were purchased from Aldrich used as received. L-Lactide(L-LA) was purchased from Aldrich and recrystallized from toluene before using. 5,10,15,20-Tetraphenylporphyrin ($TPPH_2$) was purchased from Shanghai Dibai Chemical Technology Co., Ltd. N,N′-Azobisisobutyronitrile (AIBN) was provided by Shanghai Chemical Reagent Co. used after recrystallization with 95 % ethanol. Tetrahydroxyethyl-terminated porphyrin was synthesized from tetrakis(4-hydroxylphenyl)-21H,23H-porphyrin and bromoethanol according to our previous publication [19]. Benzylsulfanylthiocarbonylsufanylpropionic acid (BSPA) was obtained according to the literature [8]. $^1$H NMR (DMSO, ppm): 2.68 (t, 2H, $CH_2$–C=O), 3.54 (t, 2H, $CH_2$–S), 4.68 (s, 2H, $CH_2$–Ph), 7.29~7.40 (m, 5H, Ph), 12.5 (b, 1H, OH). FT-IR (KBr): 1,710, 1,495, 1,451, 1,242, and 1,064 $cm^{-1}$. D-Gluconamidoethyl methacrylate glycomonomer (GAMA) was synthesized from 2-aminoethyl methacrylate hydrochloride and D-gluconolactone according to our previous publication. $^9$N,N-Dimethylformamide (DMF) and dichloromethane ($CH_2Cl_2$) were distilled from $CaH_2$ and stored under a dry nitrogen atmosphere. All other reagents and solvents were used without further purification.

### Synthesis of porphyrin-cored poly(L-LA) (SPPLA) [33, 34]

A typical experiment is as follow: the porphyrin core initiator (8.5 mg, 0.01 mmol), L-LA monomer (114.0 mg, 1.0 mmol), and the catalyst DMAP (9.8 mg, 0.08 mmol) were added to a tube. Polymerization was carried out in tetrahydrofuran (THF) at 50 °C for 24 h. Then, the resulting product was dissolved in 5 mL of dichloromethane and poured dropwise into 50 mL of cold methanol under vigorous stirring at room temperature. The precipitate was filtered and dried in vacuo at 40 °C to give 101.5 mg of the SPPLA sample (80.2 % yield).

### Preparation of SPPLA-BSPA macroRAFT agent

A typical example is given below: SPPLA (134.0 mg, 0.01 mmol), BSPA (21.7 mg, 0.08 mmol), DMAP (4.8 mg, 0.04 mmol), DCC (16.5 mg, 0.08 mmol), and 3 mL dichloromethane were added to the tube. The tube was quickly put into an oil bath at 25 °C with vigorous stirring for about 72 h. After cooling, 1 mL acetone was added into the crude product and the 1,3-dicyclohexylurea (DCU) precipitate was removed by filtration. The solvent was removed under vacuum, and then, 3 mL dichloromethane was added in order to extract the cooled polymer from the flask. Under stirring, the solution was added dropwise to 30 mL diethylether anhydrous. The product was purified by diethylether anhydrous for several times to ensure complete removal of BSPA. The precipitate was filtered and dried in vacuo at 40 °C to give 92.4 mg of the sample (67.0 % yield).

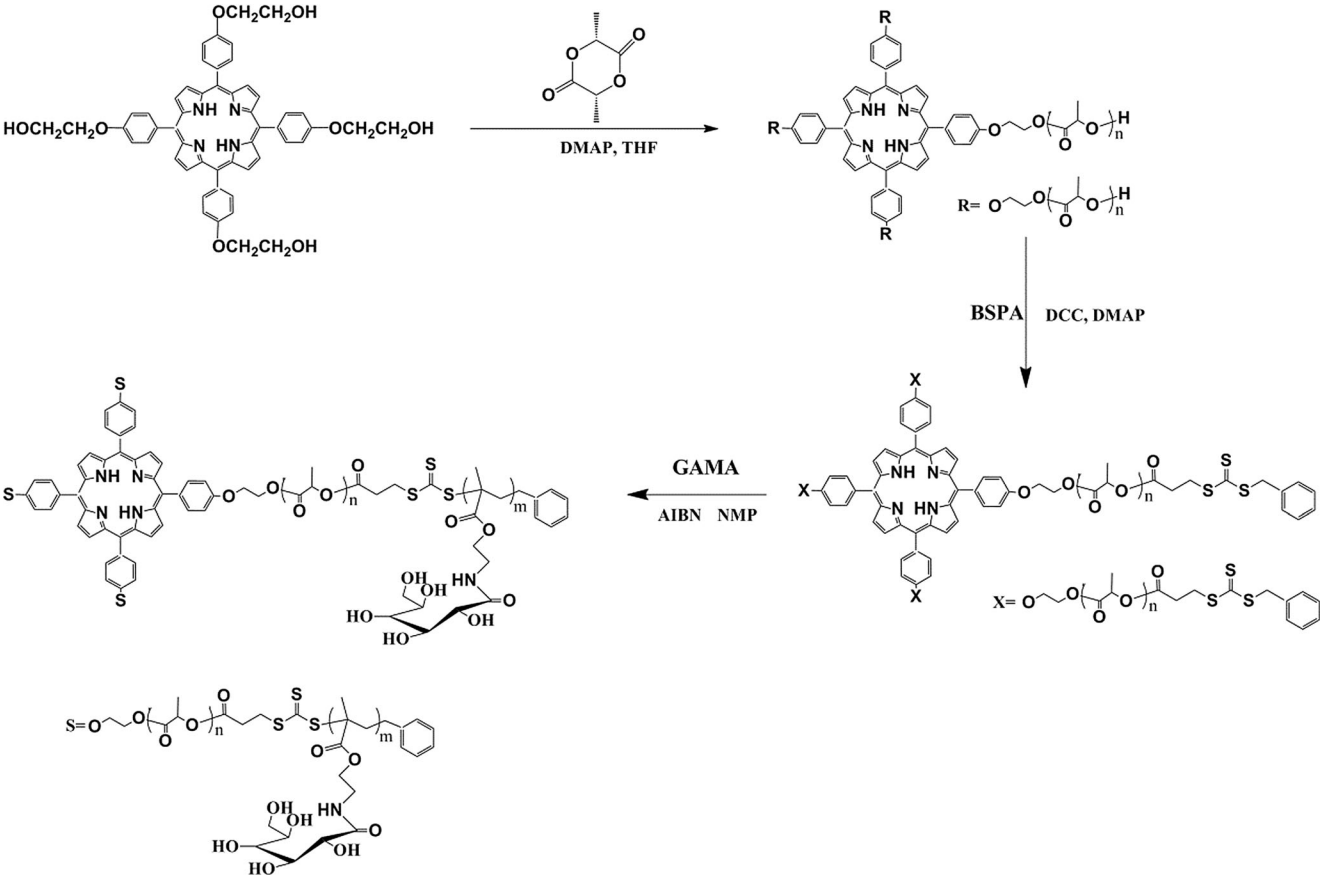


**Scheme 1** Synthesis of star-shaped porphyrin-cored SPPLA-b-PGAMA copolymers

## Preparation of star-shaped porphyrin-cored SPPLA-b-PGAMA blocks copolymer

Both SPPLA-BSPA (0.002 mmol, 28.92 mg) and GAMA glycomonomer (0.35 mmol, 107.5 mg) were dissolved in 1-methyl-2-pyrrolidinone (NMP, 0.4 mL) at room temperature, and the mixture solution was degassed with nitrogen for 15 min. AIBN (0.02 mmol, 2.9 mg) was added, and the resulting solution was degassed again for 15 min followed by stirred vigorously at 70 °C for 12 h. The crude product was precipitated into diethylether anhydrous and then purified sequentially by methanol to remove the possible GAMA homopolymer or glycomonomer. The resulting SPPLA-b-$PGAMA_{26}$ block copolymer was then dried overnight in vacuo at 40 °C (monomer conversion, 61.5 %).

## Preparation of glucose-installed aggregates in water

SPPLA-b-$PGAMA_4$ and SPPLA-b-$PGAMA_{26}$ copolymer was dissolved in DMF (1 mg/mL), and distilled water was then added gradually at a speed of 10 μL/min using a microsyringe. After stirring for 24 h, with a dialyzing method, DMF was completely removed and the morphology of aggregates was determined by transmission electron microscopy (TEM).

## Measurement of the critical aggregation concentration of SPPLA-b-PGAMA

Using DPH as a probe molecule, the critical aggregation concentration (cac) of SPPLA-b-$PGAMA_4$ and SPPLA-b-$PGAMA_{26}$ copolymers was measured [35]. DPH was dissolved in methanol to produce 0.5 mM DPH methanol solution, and then, 5-μL DPH solutions were added to containers and the methanol was allowed to evaporate. Each aqueous sample solutions with various polymer concentrations from $10^{-5}$ to 0.5 mg/mL containing the same concentration of excess DPH residue were obtained. UV–vis spectra of samples were recorded at 313 nm range at room temperature.

## Lectin recognition

The lectin recognition experiment of the SPPLA-b-$PGAMA_{26}$ copolymer solution was studied by changes in the turbidity of solution with time at 360 nm with different aggregate solution into ConA solution, and the concentration of ConA was 0.5 mg/mL.

### Determination of the fluorescence quantum yield

Fluorescence quantum yield of SPPLA-b-PGAMA$_{26}$ was obtained from the formula (1) and formula (2) with TPPH$_2$ as the standard (fluorescence quantum yield $\Phi$=0.11) [36–39]. Both concentration of TPPH$_2$ and SPPLA-b-PGAMA$_{26}$ were 1.63 μmol L$^{-1}$.

$$\Phi = 0.11\frac{A_{\mathrm{TPPH2}}\, S_{\mathrm{SPPLA\text{-}b\text{-}PGAMA26}}}{S_{\mathrm{TPPH2}}\, A_{\mathrm{SPPLA\text{-}b\text{-}PGAMA26}}} \quad (1)$$

$$S = \int_{\lambda 600\mathrm{nm}}^{\lambda_{800\mathrm{nm}}} I_{\mathrm{f}\,\lambda}\mathrm{d}\lambda \quad (2)$$

where $A_{\mathrm{TPPH2}}$: TPPH$_2$ in absorbance at 425 nm; $S_{\mathrm{TPPH2}}$: reference sample TPPH$_2$ integral area of the fluorescence emission spectra from 600 to 800 nm ($E_X$=425 nm); $A_{\mathrm{SPPLA\text{-}b\text{-}PGAMA26}}$: SPPLA-b-PGAMA$_{26}$ in absorbance at 425 nm absorbance; $S_{\mathrm{SPPLA-PGAMA26}}$: fluorescence emission spectra of integral area from 600 to 800 nm ($E_X$= 425 nm); and $I_{\mathrm{f}\,\lambda}$: fluorescence emission curve of TPPH$_2$ or SPPLA-b-PGAMA$_{26}$.

### Detecting singlet oxygen ($^1O_2$) production

In our study, 1,3-diphenylisobenzofuran (DPBF) was proposed to detect $^1O_2$ generated by SPPLA-b-PGAMA photosensitizers (TPPH$_2$ as the standard regent) [8, 39, 40]. DPBF can react with $^1O_2$ irreversibly, which induces a decrease in the fluorescence intensity of the DPBF absorption band at 456 nm. In a typical experiment, 150 μL TPPH$_2$ (0.147 mM) or SPPLA-b-PGAMA$_{26}$ (0.147 mM) was mixed with 3 mL of DPBF (2.5 μM) in DMF, respectively. The solutions were irradiated with a 650-nm laser source (5 mW), and their fluorescence intensities at 456 nm were recorded every 1 min in a luminescence spectrometer. The singlet oxygen quantum yield ($\eta$) of SPPLA-b-PGAMA$_{5000}$ in DMF was calculated using the following equation [41, 42]:

$$\eta = \Phi_{\mathrm{TPPH2}}\frac{t_{\mathrm{TPPH2}}}{t_{\mathrm{SPPLA\text{-}b\text{-}PGAMA}}} \quad (3)$$

where $t_{\mathrm{TPPH2}}$ is the time for decrease in absorption of DPBF in the presence of TPPH$_2$ free in DMF solution adjusted to a first-order exponential decay and $t_{\mathrm{SPPLA\text{-}b\text{-}PGAMA}}$ is the time for decrease in absorption of DPBF in the presence of SPPLA-b-PGAMA$_{26}$ in DMF adjusted to a first-order exponential decay. The singlet oxygen quantum yield TPPH$_2$ free in DMF solution is 0.67±0.09.

### Cell culture

Briefly, COS-7 (a kidney cell line of the African green monkey) and BEL-7402 cells (a cell line derived from human hepatoma) were grown at 37 °C with 5 % $CO_2$ environment. Dulbecco's modified Eagle's medium (DMEM) with 10 % fetal bovine serum (FBS), penicillin (100 U/ml), and streptomycin (100 U/mL) were used. Cells were sub cultured every 2–3 days.

### Cell viability assay

The relative cytotoxicity of SPPLA-b-PGAMA$_{26}$ was estimated by standard MTT method. COS-7 cells were seeded in 96-well plates at a density of 9,000 cells/well. The cells were cultured for 24 h, and then, DMEM was replaced with fresh 200 μL medium. Fifty microliters of phosphate-buffered saline (PBS) containing serial concentrations of SPPLA-b-PGAMA solutions filtered through a Millipore filter (pore size, 0.22 μm) was added in corresponding wells to get final SPPLA-b-PGAMA$_{26}$ concentrations of 12, 23, 45, 90, and 180 μg/mL. After the cells were incubated for 24 h, stock reagents of 25 μL MTT (5 mg/mL) were added into every well. Four hours later, the medium was removed carefully. Two hundred microliters of DMSO was used in every well to dissolve formazan crystals, and the optical density at the wavelength of 490 nm ($OD_{490}$) was recorded by BioTech System. The cell survival ratios were converted by the formula as follows:

$$\text{cell viability} = \left([\mathrm{OD}_{490}]_{\mathrm{sample}}/[\mathrm{OD}_{490}]_{\mathrm{control}}\right) \times 100\%$$

### In vitro antitumor evaluation

The 96-well plates were used and BEL-7402 cells were seeded at a density of 9,000 cells/well. The cells were cultured for 24 h, and then, various concentrations of SPPLA-b-PGAMA$_{26}$ solution with DMEM were prepared and filtered through a Millipore filter (pore size, 0.22 μm). Exposed to different doses of light (2 W, 5 and 10 min), appropriate solution was added to get SPPLA-b-PGAMA$_{26}$ solution at different concentrations (12, 23, 45, 90, and 180 μg/mL). The subsequent procedures were the same as those described in the cell viability assay. The cell inhibition efficiency was calculated by the formula as follows:

$$\text{cell survival} = \left([\mathrm{OD}_{526}]_{\mathrm{sample}}/[\mathrm{OD}_{526}]_{\mathrm{control}}\right) \times 100\%$$

### Instrumentation

Nuclear magnetic resonance spectroscopy (NMR) spectra were recorded at room temperature on a Varian Mercury-400 spectrometer. $CDCl_3$, DMSO-$d_6$, and $D_2O$ were used as the

deuterated solvents for the SPPLA precursors and SPPLA-b-PGAMA block copolymers.

Gel permeation chromatography (GPC) was determined on GPC (Perkin-Elmer Series 200) and a refractive index detector at 30 °C. The elution phase was DMF (0.01 mol/L LiBr) (elution rate, 1.0 mL/min), and polystyrene was used as the calibration standard.

Transmission electron microscope (TEM) micrographs were taken with a JEOL-JEM-2010 (JEOL, Japan) operated at 200 kV. One drop of aggregates solution was deposited onto the surface of 300 mesh formvar–carbon film-coated copper grids. Excess solution was quickly wicked away with a filter paper. The image contrast was enhanced by negative staining with phosphotungstic acid (0.5 wt.%).

The differential scanning calorimetry (DSC) analysis was carried out using a Perkin-Elmer Pyris 1 instrument under nitrogen flow (10 mL/min). All samples were heated from 0 to 160 °C at 10 °C/min.

Dynamic light scattering (DLS) was determined by using a Malvern Nano_S instrument (Malvern, UK). The solution of aggregates was performed at a scattering angle of 90° and at 25 °C.

Fluorescent spectra were performed at room temperature using a luminescence spectrometer (Cary Eclipse, Australia). Fluorescence quantum yield test was performed at room temperature in the range of 600–800 nm using an increment of 5 nm and an excitation wavelength of 425 nm, while singlet oxygen detection was performed at room temperature in the range of 425–600 nm using an increment of 5 nm and an excitation wavelength of 403 nm.

The optical density (OD) value was measured at 490 or 526 nm by Microplate Reader (Thermo Fisher Scientific).

**Table 1** Synthesis of star-shaped porphyrin-cored poly(L-lactide) (SPPLA) using a hydroxyl-terminated porphyrin initiator and DMAP catalyst in THF at 50 °C

| Entry | [*M*]/[*I*][a] | [*I*]/DMAP | $M_{n,GPC}$ | $M_{n,th}$[b] | $M_{n,NMR}$[c] | $M_w/M_n$[d] | Yield (%) |
|---|---|---|---|---|---|---|---|
| SPPLA | 80/1 | 1/8 | 13,950 | 10,070 | 11,700 | 1.25 | 80.2 |
| SPPLA2 | 120/1 | 1/8 | 17,540 | 14,330 | 16,320 | 1.41 | 78.9 |
| SPPLA3 | 160/1 | 1/8 | 20,890 | 19,060 | 22,170 | 1.29 | 79.7 |
| SPPLA4 | 200/1 | 1/8 | 25,560 | 25,910 | 27,350 | 1.29 | 87.3 |
| SPPLA5 | 240/1 | 1/8 | 29,110 | 27,810 | 33,110 | 1.30 | 78.6 |

[a] *M* L-lactide monomer, *I* initiator

[b] $M_w/M_n$ denotes the molecular weight distribution of polymer, where weight-average molecular weight ($M_w$) and number-average molecular weight ($M_n$) are determined by GPC

[c] $M_{n,th}=[M]/[I]\times M_{monomer}\times$yield$+M_{initiator}$, $M_{n,th}$ denotes the theoretical number-average molecular weight of the SPPLA polymers

[d] $M_{n,NMR}$ was determined from the integral ratio of the signals on the main chain of polymer ($-CH(CH_3)$, $\delta H^b$ =5.00–5.30 ppm) and the signals on lactyl end group ($HOCH(CH_3)CO$, $\delta H^{b'}$ =4.36 ppm): $M_{n,NMR}=M_{initiator\ residue}+\delta H^b/\delta H^{b'}\times 72\times$arm number

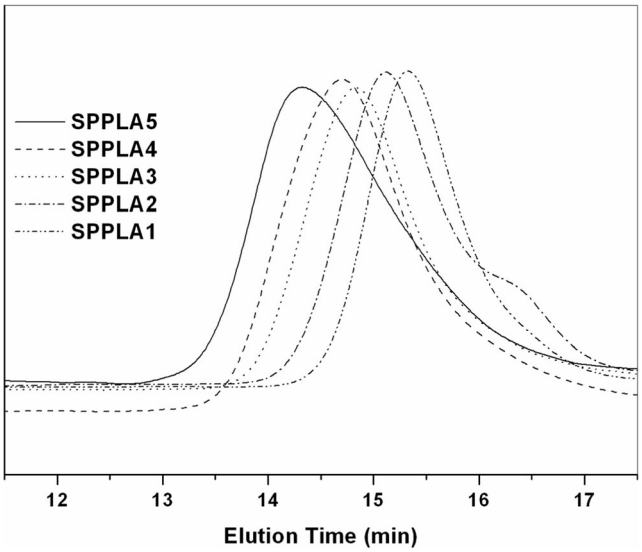


**Fig. 1** GPC traces of the SPPLA samples

## Results and discussion

### Synthesis of star-shaped porphyrin-cored SPPLA

In this work, we utilized tetrahydroxyethyl-terminated porphyrin as the core initiator and DMAP as the catalyst to synthesize a family of SPPLA polymers (Table 1, Fig. 1). At different times, the GPC curves represent symmetrical elution peaks and the molecular weight distribution ($M_w/M_n$) is relatively narrow, which suggests a progressing of the polymer molecular weight (Fig. 2). Moreover, the polymer molecular weight obtained by $^1$H NMR ($M_{n,NMR}$) has a good consistency with the theoretical molecular weight of polymer ($M_{n,th}$)($M_{n,th}=[M]/[I]\times M_{monomer}\times$yield$+M_{initiator}$). This suggests that the molecular weights of the SPPLA polymers could be precisely predicted changing the molar ratio of initiator to monomer. As a note, $M_{n,th}$ is significantly lower than $M_{n,GPC}$ because of the different hydrodynamic volume of SPPLA

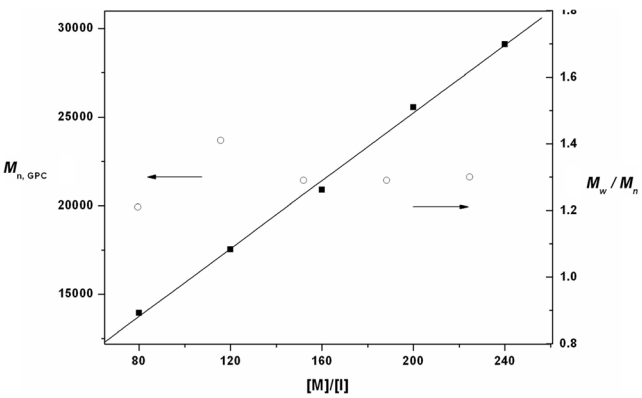


**Fig. 2** Dependence of $M_{n,GPC}$ on the molar ratio of [*M*]/[*I*] with tetrahydroxyl terminated porphyrin core initiator and DMAP catalyst in THF at 50 °C

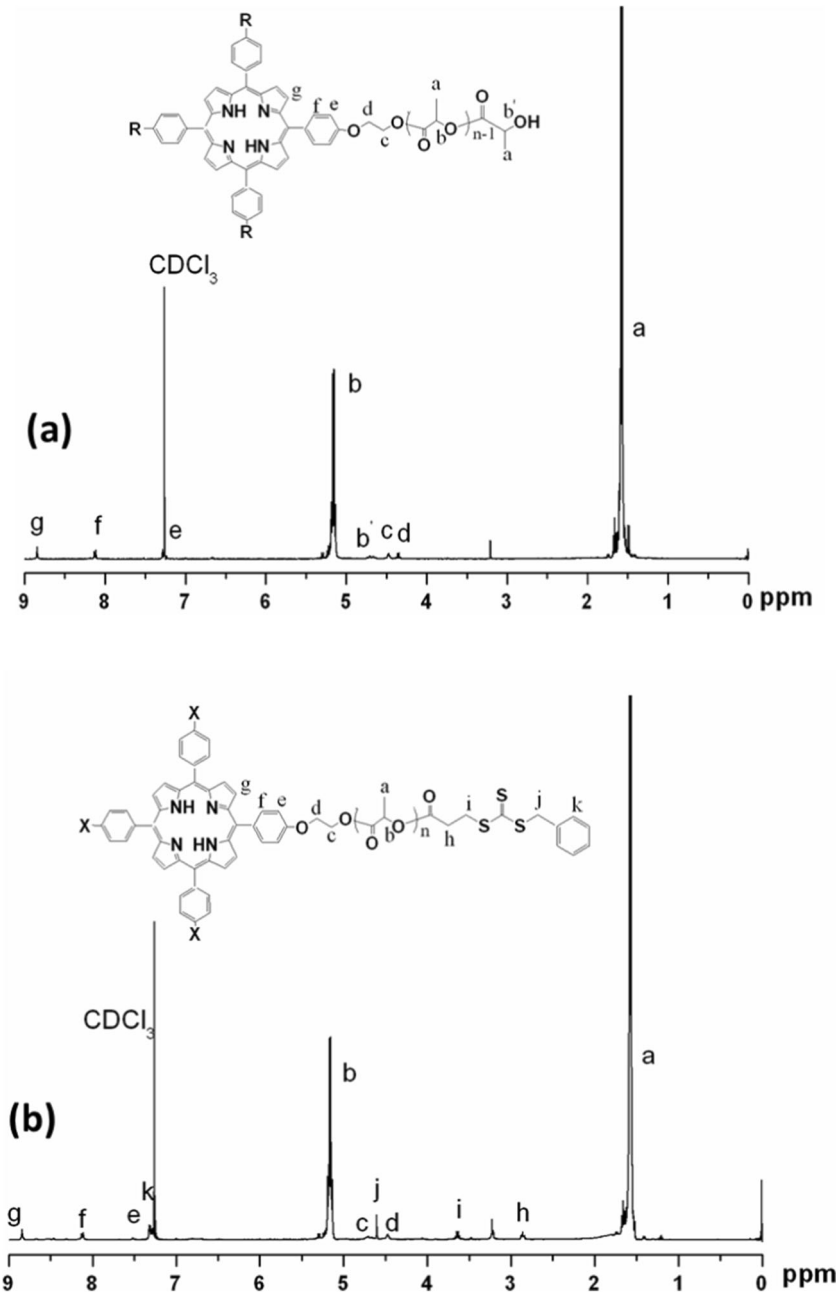


**Fig. 3** $^{1}$H NMR spectra of SPPLA (**a**) and macroRAFT agent SPPLA-BSPA (**b**) in $CDCl_3$

polymers when used polystyrene as a calibration standard for GPC characterization.

Compared with porphyrin initiator, the $^{1}$H NMR spectrum of SPPLA polymer is shown (Fig. 3). Besides the typical proton signals at 1.40–1.75 ($\delta H^{a}$) and 5.10–5.35 ppm ($\delta H^{b}$) of its main chain, proton signals on the end group (4.68 ppm HO***CH***($CH_3$)CO, $\delta H^{b'}$) and the protons on the methyleneoxy groups belong to the porphyrin initiator 4.33–4.39 ppm (PhO***CH$_2$***$CH_2$O, $\delta H^{d}$) and 4.44–4.52 ppm (PhO$CH_2$***CH$_2$***O, $\delta H^{c}$). In addition, proton signals of porphyrin core initiator was shown at 7.26–7.32 ppm ($\delta H^{e}$), 8.08–8.15 ppm ($\delta H^{f}$), and 8.80–8.88 ppm ($\delta H^{g}$), and carboxylic acid proton signals could not be detected [43]. In all, it can be indicated that well-defined SPPLA polymers were successfully obtained from the ROP of L-LA using tetrahydroxyethyl-terminated porphyrin initiator and DMAP catalyst in THF at 50 °C.

## Preparation of biomimetic star-shaped porphyrin-cored SPPLA-b-PGAMA block copolymers

To date, varieties of glycopolymer are synthesized by controlled polymerization techniques such as ROP [44], nitroxide-mediated radical polymerization (NMP) [45], atom transfer radical polymerization (ATRP) [46], and reversible addition-fragmentation chain transfer polymerization (RAFT) [47]. In this study, star-shaped porphyrin-cored SPPLA-b-

**Table 2** Synthesis of biomimetic star-shaped porphyrin-cored SPPLA-b-PGAMA block copolymers via the RAFT of GAMA Monomer in NMP solution at 70 °C

| Entry[a] | [AIBN]/[Macro-RAFT] | [GAMA]/[I] | Monomer conv. (%) | $f_{PLA}/f_{PGAMA}$[b] (%/%) | $M_{nGPC}$[c] | $M_w/M_n$[d] | $M_{n,NMR}$[e] |
|---|---|---|---|---|---|---|---|
| SPPLA-BSPA | 0 | 0 | 80.0 | 100/0 | 13,950 | 1.54 | 12,720 |
| SPPLA-b-PGAMA$_4$ | 1.2 | 40 | 61.5 | 72.1/27.9 | 20,510 | 1.74 | 17,650 |
| SPPLA-b-PGAMA$_{26}$ | 1.2 | 220 | 65.2 | 28.9/71.1 | 32,770 | 1.48 | 43,980 |

[a] The subscript numbers represent the repeating units of polymers

[b] *f* denotes the weight fractions of PLA and/or PGAMA within block copolymers, which was determined by $^1$H NMR

[c] Weight-average molecular weight ($M_w$) and number-average molecular weight ($M_n$) are determined by GPC

[d] $M_w/M_n$ denotes the molecular weight distribution of polymer, where weight-average molecular weight ($M_w$) and number-average molecular weight ($M_n$) are determined by GPC in DMF

[e] $M_{n,NMR}$ was determined from the integral ratio of the signal on the main chain of PLA (−CH−, 5.07–5.37 ppm) and the signal on the main chain of PGAMA (−$CH_2$−, 1.77–2.00 ppm) from the $^1$H NMR spectra

PGAMA block copolymers were successfully prepared by the RAFT of unprotected GAMA in polar NMP solvent at 70 °C (Scheme 1). Firstly, we used SPPLA which reacted with BSPA, and macroRAFT agent of SPPLA-BSPA was obtained. The typical methine signal of the SPPLA end group at 4.68 ppm (HO***CH***($CH_3$)CO, $\delta H^{b\prime}$) completely disappeared, and new proton signals at 2.80–2.90, 3.51–3.71, and 4.56–4.64 ppm which belonged to the trithiocarbonate unit in BSPA were observed. In addition, the integral ratio of the methyleneoxy group proton signals to methylene end group has a good consistency with theoretical value ($H^d/H^j$)=2.0/2.01) (Fig. 3). These results prove that the SPPLA with hydroxyl end groups was indeed converted into SPPLA-BSPA with trithiocarbonate end groups.

Then, with SPPLA-BSPA as the macroRAFT agent, two different units of GAMA glycomonomer of star-shaped porphyrin core SPPLA-b-PGAMA were synthesized (Table 2). Compared with that of the SPPLA, the molecular weight distribution ($M_w/M_n$) is narrow and, at different elution times, the GPC curves showing symmetrical elution peaks, which indicate a progressing of the polymer molecular weight (Fig. 4). Moreover, the actual copolymer molecular weight calculated by $^1$H NMR ($M_{n,NMR}$) increases linearly when changing molar ratio of GAMA glycomonomer to SPPLA-BSPA ([GAMA]/[SPPLA-BSPA]). This suggests that the molecular weights of the SPPLA polymers could be precisely predicted by changing the molar ratio of initiator to monomer, which is a typical feature of "living"/controlled radical polymerization. However, it is should be noted that the monomer conversion of GAMA is relatively low (about 65 %), which might be attributed to the steric hindrance around the propagating radical of GAMA [48, 49].

Compared with the SPPLA-BSPA macroRAFT agent, the $^1$H NMR of SPPLA-b-PGAMA copolymers clearly appears that besides the typical proton signals of SPPLA backbone, some new proton signals could be observed at 4.00–4.62 ppm for glucose residues, and the proton signals of backbone of PGAMA glycopolymer are shown at 1.85–1.95 and 0.70–1.00 ppm (Fig. 5). Moreover, the DSC measuring results of the SPPLA-b-PGAMA copolymers showed that the crystallization of the SPPLA was significantly inhibited by the outer PGAMA blocks, and with increased block units of PGAMA, the crystallinity (Xc) of the SPPLA block within copolymers decreased significantly from 25.4 to 7.0 %, which was shown in Table 3 and Fig. S1. This suggests that the crystallization of the inner SPPLA block could be inhibited progressively by the outer PGAMA block that will improve the compatibility of hydrophobic SPPLA block for drug delivery [19, 31, 50].

## UV–vis analyses

The obtained SPPLA-b-PGAMA copolymers were further characterized using UV–vis spectroscopy (Fig. 5). As the same as porphyrin, in the UV–vis, the soret (435 nm) and Q

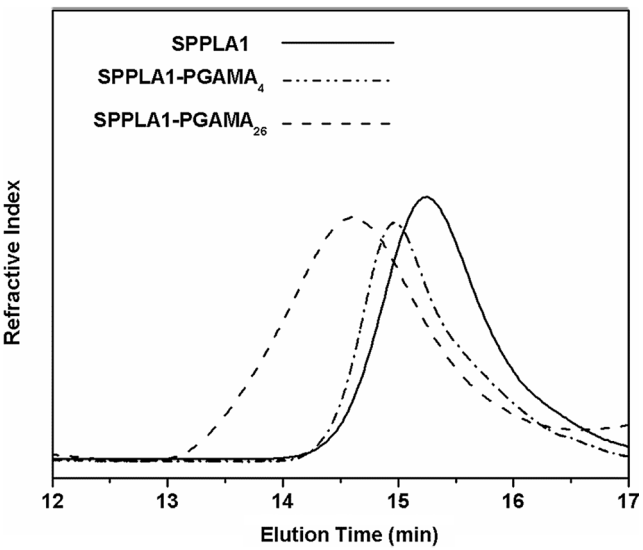


**Fig. 4** GPC traces of the as-synthesized SPPLA-b-PGAMA copolymer and SPPLA

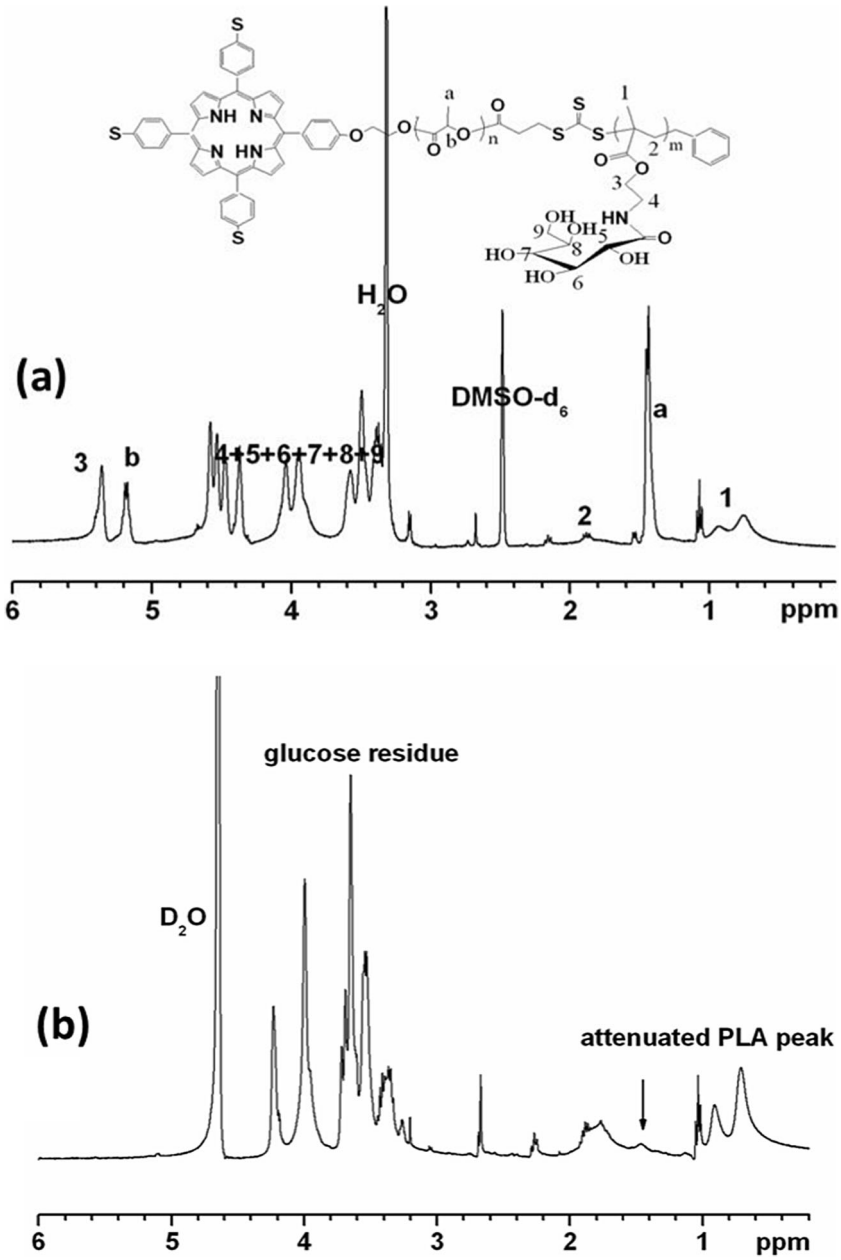


**Fig. 5** $^{1}$H NMR spectra of SPPLA-b-PGAMA block copolymers in $d_6$-DMSO (**a**) and $D_2O$ (**b**)

**Table 3** Thermal properties of star-shaped porphyrin-cored SPPLA-b-PGAMA block copolymers

| Entry | $T_m$ [a] (°C) | $\Delta H_m$ [b] (J/g) | $X_c$ [c] (%) |
|---|---|---|---|
| SPPLA | 139.1 | 19.9 | 25.4 |
| SPPLA-b-PGAMA$_4$ | 128.5, 132.4 | 8.0 | 11.8 |
| SPPLA-b-PGAMA$_{26}$ | 127.7 | 1.9 | 7.0 |

[a] $T_m$ denotes the maximal melting temperature of SPPLA block within copolymer in the heating run

[b] $\Delta H_m$ denotes the fusion enthalpy of SPPLA block within copolymer in the heating run

[c] $X_c$ denotes the degree of crystallization of SPPLA block within copolymer, and $X_c = \Delta H_m/(f \times \Delta H^0_{m,PLA})$, $\Delta H^0_{m,PLA} = 93.6$ J/g

bands (500–700 nm) SPPLA-b-PGAMA were shown to have belonged to porphyrin. This proves that porphyrin moiety still retained the luminescent property within SPPLA-b-PGAMA. Thus, this will potentially enable SPPLA-b-PGAMA for the biological probe and PDT applications [51].

## Self-assembly of biomimetic star-shaped porphyrin-cored SPPLA-b-PGAMA block copolymers

Using a dialysis method, the glycopolymer-installed and SPPLA-cored nanoparticles were prepared through a self-assembly way in aqueous solution [43]. The $^{1}$H NMR of SPPLA-b-PGAMA$_{26}$ copolymer in $D_2O$ solution showed

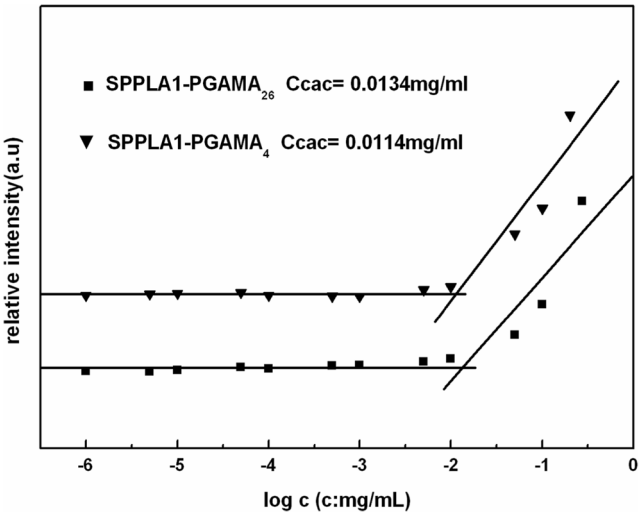


**Fig. 6** The relationship of the absorbance intensity of DPH as a function of SPPLA-b-PGAMA block copolymer concentration at room temperature

the decreased proton signals of hydrophobic SPPLA block compared with that in solvent of $d_6$-DMSO (Fig. 5). The reason was attributed to the attenuated mobility of SPPLA blocks and the shielding effect of hydrophilic PGAMA shell. This also suggests the spontaneous self-assembly of SPPLA-b-PGAMA copolymers in aqueous solution.

Then, the dye solubilization method was used to examine SPPLA-b-PGAMA copolymers' critical aggregation concentration (cac) [43]. The cac was an important parameter for the thermodynamic stability of self-assembled aggregates in aqueous solution. In our experiment, the agent of DPH was employed as a probe regent, meanwhile the relationship of the absorbance intensity of DPH as a function of copolymer concentration at room temperature is shown. The absorbance intensity values of DPH keep consistent below a certain concentration (Fig. 6). Above that concentration, the absorbance intensity increased dramatically indicating that the DPH was incorporated into the hydrophobic region of aggregates. When the block length of PGAMA increased, the cac value of SPPLA-b-PGAMA copolymers slightly increased from 0.0114 to 0.0134 mg/mL which has a similar conclusion to other reports about amphiphilic copolymers [35].

TEM was employed to study the morphology of the self-assembled aggregates from these two SPPLA-b-$PGAMA_4$ and SPPLA-b-$PGAMA_{26}$ copolymers (Fig. 7). For investigating the influence of PGAMA block length on the morphology of aggregates, the hydrophobic SPPLA block was kept at 19 repeating unit. In Fig. 7a, with a relatively long hydrophilic PGAMA (e.g., SPPLA-b-$PGAMA_{26}$, $f_{PGAMA}$=71.9 %), it can be seen that the normally spherical micelles were observed. While in case of the short PGAMA, block worm-like aggregate morphologies were mainly observed for SPPLA-b-$PGAMA_4$ block copolymer [$f_{PGAMA}$=27.9 %] (Fig. 7b). This phenomenon could be induced by the decreased repulsion among the corona chains (i.e., hydrophilic PGAMA corona) and the increased surface tension resulting from the increased hydrophobicity–hydrophilicity balance. It can be concluded that different aggregate morphologies can be formed through adjusting PGAMA weight fraction within the copolymers which has a very similar conclusion on the polymeric aggregate morphological transformation, as reported for biodegradable poly(L-LA)—and/or PCL-b-poly(ethylene oxide) copolymers [35, 52, 53]. Significantly, it is a good method to fabricate targeted drug delivery systems.

## Fluorescence quantum yield [37]

Based on formula (1) and formula (2), the fluorescence quantum yield of SPPLA-b-$PGAMA_{26}$ was 0.22, which proves that these porphyrin core star-shaped block copolymers possess high fluorescence quantum yields. Porphyrin derivatives have been demonstrated to influence the chemistry and photophysics of molecules by altering the microenvironment in which the molecules reside, so the reason could be attributed to the fact that porphyrin as the core being surrounded by the armed copolymer resulting in high steric hindrance which can prevent self-aggregation and self-quenching of the central porphyrin.

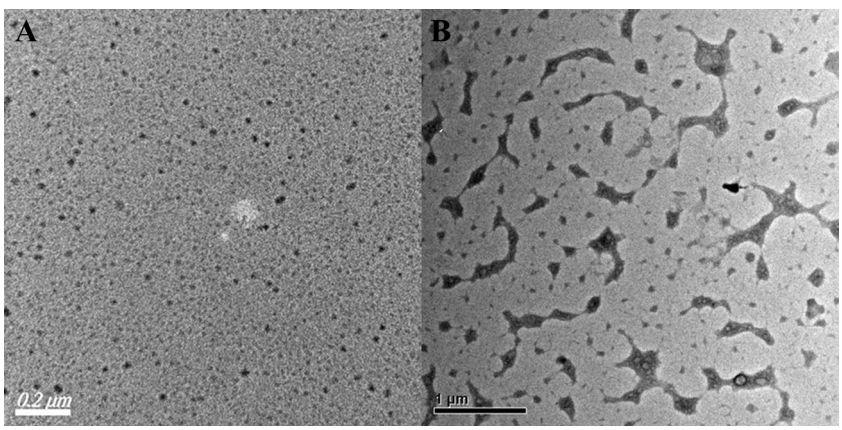


**Fig. 7** TEM photographs of copolymers SPPLA-b-$PGAMA_{26}$ (**a**) and SPPLA-b-$PGAMA_4$ (**b**)

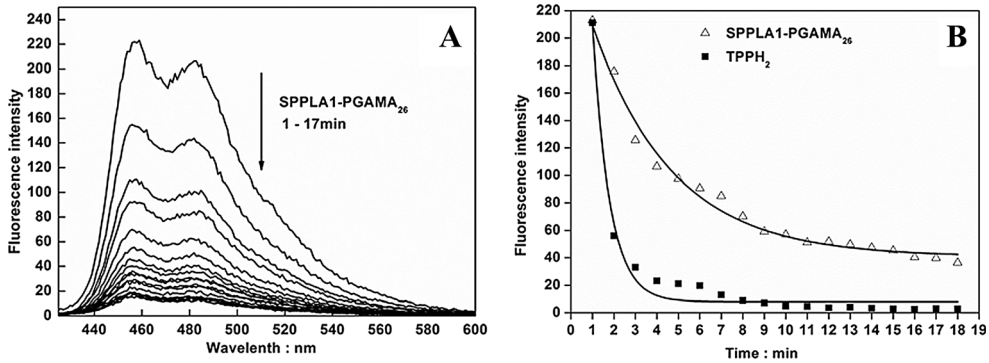


**Fig. 8** Fluorescence intensity decay curves of DPBF with SPPLA-b-PGAMA$_{26}$ or TPPH$_2$ as function of time with a laser source (650±10 nm, 5 Mw) (**a**) and fluorescence intensity at 456 nm decay curves of DPBF with SPPLA-PGAMA$_{26}$ or TPPH$_2$ (**b**)

## Singlet oxygen ($^1O_2$) production of SPPLA-b-PGAMA plus irradiation

$^1O_2$ is the prerequisite molecule in the PDT. DPBF, which was used as a chemical photosensitizer in this study to detect the production of singlet oxygen, reacts irreversibly with $^1O_2$ resulting into a decreased intensity of the DPBF fluorescence absorption band at ~400 nm. The decrease in fluorescence intensity at 456 nm as a function of irradiation time was shown (Fig. 8). According to the reported singlet oxygen generation estimation method, the singlet oxygen release delivery ($\eta$) by a suspension of porphyrin-cored SPPLA-b-PGAMA$_{26}$ is estimated to be 0.15, while the photofrin with singlet oxygen quantum yield less than 0.3 as a sensitizer has been used as a PDT agent in clinical trial [54]. This result suggests that the SPPLA-b-PGAMA$_{26}$ presented here is an interesting candidate as PDT agents. Moreover, in the case of free porphyrin TPPH$_2$, the fluorescence intensity of DPBF caused by TPPH$_2$ dropped sharply to 20 % in 2 min which proves a large number of singlet oxygen produced during this period; however, the fluorescence intensity of DPBF declined slowly when mixed with SPPLA-b-PGAMA$_{26}$. In other words, the singlet oxygen production ability of SPPLA-b-PGAMA$_{26}$ can be well controlled by irradiation time, which indicates that this will be a promising technology for PDT [55, 56].

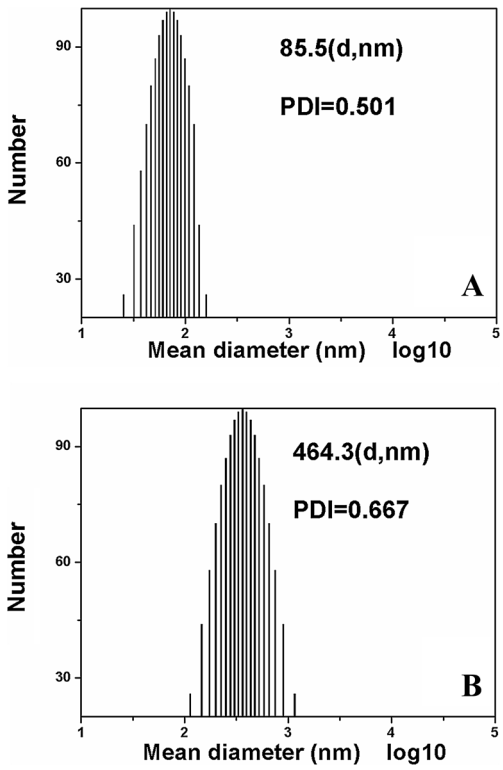


**Fig. 9** Nanoparticles size distribution of the SPPLA-b-PGAMA $_{26}$ ($C_{copolymer}$=0.1 mg/mL) (**a**) and SPPLA-b-PGAMA$_{26}$-ConA ($C_{copolymer}$=0.1 mg/mL, $C_{ConA}$=0.5 mg/mL) (**b**) in aqueous solution at room temperature

## Recognition measurement of SPPLA-b-PGAMA block copolymers

In living systems, the pathological and psychological process was governed by the sugar–protein recognition events that will provide a promising application for biomaterials applications and drug discovery. It has been reported that ConA could specifically recognize D-mannopyranoside and D-glucopyranoside residues with free 3-, 4-, and 6-hydroxyl groups, which usually can result in the ConA-cross-linked aggregates [11, 26, 51, 52]. In this study, the interaction of

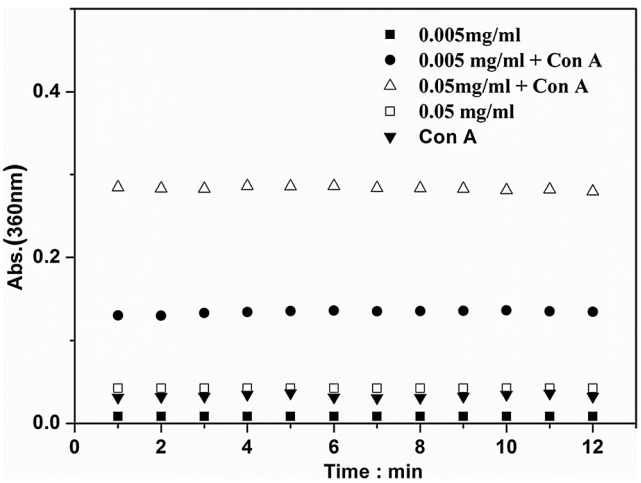


**Fig. 10** Interactions of ConA (0.5 mg/mL) with SPPLA-b-PGAMA$_{26}$ at different concentrations

SPPLA-b-PGAMA$_{26}$ copolymer with ConA was a measurement in aqueous solution. The turbidity has a slightly increase with the copolymer concentration for SPPLA-b-PGAMA$_{26}$ sample, and there is no precipitation could be observed. This phenomenon implies that the linking between ConA and copolymer may occur and caused ConA-cross-linked aggregates that clarified by the DLS analysis. Compared with the average size of the original copolymer aggregates (about 85.5 nm), the ConA-cross-linked aggregates (about 464.3 nm) were significantly increased (Fig. 9). Measured by UV–vis, it is suggested that the ConA-cross-linked aggregates would keep stable in aqueous solution and the turbidity would not dramatically change (Fig. 10). In all, the above analyses prove that the SPPLA-b-PGAMA$_{26}$ copolymers indeed specifically linked with ConA in aqueous solution which suggested that this porphyrin-cored star-shaped SPPLA-b-PGAMA could be applied in targeted drug delivery system.

## Cytotoxicity and photo-toxicity of SPPLA-b-PGAMA micelles

Low toxicity is very important for the biomedical application of polymeric materials. Based on the MTT assay, the cell viability of SPPLA-b-PGAMA$_{26}$ was evaluated against COS-7 cells. It was shown that SPPLA-b-PGAMA$_{26}$ was not affected by the incubation with the concentration of copolymer up to 180 μg/mL, which proves that SPPLA-b-PGAMA could be a promising material for clinical use (Fig. 11). Considering that many natural polysaccharides exhibit good biological activities, the antitumor ability of SPPLA-b-PGAMA was evaluated by MTT assay against BEL-7402 cancer cells. It shows that SPPLA-b-PGAMA$_{26}$ can inhibit the growth of cancer cells because when the irradiation time was extended from 5 to 10 min, more cancer cells die, which proves that light plays a key role for porphyrin in PDT (Fig. 12), so the SPPLA-b-PGAMA could play an important contribution for the therapeutic efficacy. However, it should be noted that because of relatively low SPPLA-b-PGAMA concentration, the antitumor effect is in need of being improved.

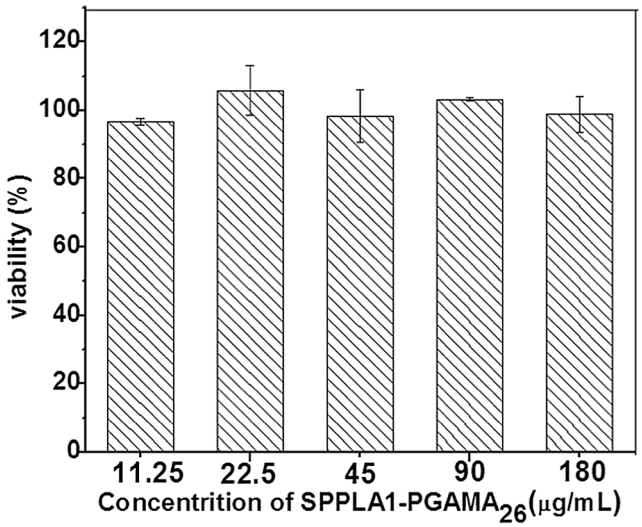


**Fig. 11** In vitro cytotoxicity of SPPLA-b-PGAMA$_{26}$ with different concentrations to COS-7 cells after 24 h incubation (mean ± SD, $n$=3)

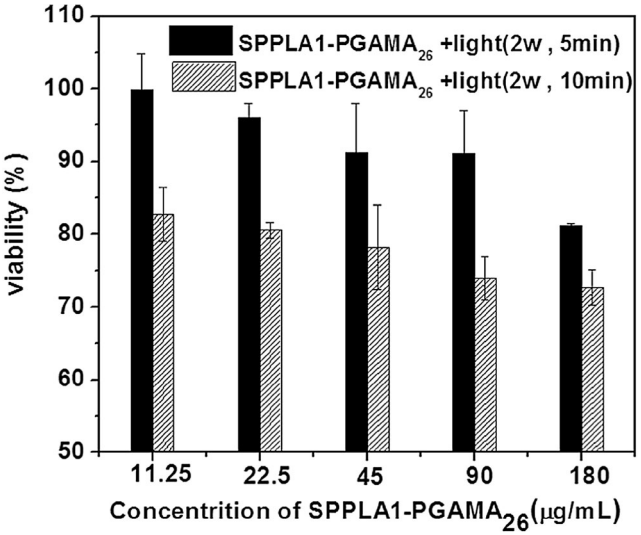


**Fig. 12** SPPLA-b-PGAMA$_{26}$ in BEL-7402 cells with different irradiation time

## Conclusions

Star-shaped porphyrin-cored SPPLA-b-PGAMA block copolymers were successfully synthesized from the direct RAFT of unprotected GAMA glycomonomer using SPPLA-BSPA as a macroRAFT agent in NMP solution at 70 °C. When the hydrophilic PGAMA block increased, the morphology of the aggregates changed from worm-like aggregates to spherical micelles. Moreover, such SPPLA-b-PGAMA copolymer exhibits efficient singlet oxygen generation and indicates high fluorescence quantum yields. Furthermore, these SPPLA-b-PGAMA copolymers showed specific recognition with ConA because of stable ConA-cross-linked aggregates in aqueous solution. MTT results showed that when given a longer irradiation time, more MCF-7 cells died. Particularly, these star-shaped porphyrin-cored SPPLA-b-PGAMA block copolymers provide a potential for targeted PDT.

**Acknowledgments** The authors are greatly grateful for the financial support of the National Natural Science Foundation of China (21004031), the Natural Science Foundation of Jiangsu Province (BK2011459), the National Postdoctoral Foundation of China (20090461065), the National Postdoctoral Foundation of Jiangsu Province (1001034B), Open Foundation of Stake Key Laboratory of Natural and Biomimetic Drugs, Peking University (K20110105), and the social development Foundation of Zhen jiang (SH2012024).

## References


1. Huang Z (2005) Technol Cancer Res Treat 4:283
2. Anand S, Ortel BJ, Pereira SP, Hasan T, Maytin EV (2012) Cancer Lett 326:8–16
3. Dolmans DE, Fukumura D, Jain RK (2003) Nat Rev Cancer 3:380
4. Snyder JW, Greco WR, Bellnier DA, Vaughan L, Henderson BW (2003) Cancer Res 63:8126
5. Zhang XM, Wu HS, Chen XM (2003) Eur J Inorg Chem 2003:2959
6. Nishiyama N, Stapert HR, Zhang GD et al (2003) Bioconjug Chem 14:58
7. Dai X-H, Zhang H-D, Dong C-M (2009) Polymer 50:4626
8. Peng C-L, Shieh M-J, Tsai M-H, Chang C-C, Lai P-S (2008) Biomaterials 29:3599
9. Dai XH, Dong CM (2008) J Polym Sci A Polym Chem 46:817
10. Murariu M, Ferreira AD, Alexandre M, Dubois P (2008) Polym Adv Technol 19:636. doi:10.1002/pat.1131
11. Hu Y, Hu Y, Topolkaraev V, Hiltner A, Baer E (2003) Polymer 44: 5711
12. Jiang L, Wolcott MP, Zhang J (2006) Biomacromolecules 7:199
13. Cohn D, Hotovely-Salomon A (2005) Polymer 46:2068
14. Maglio G, Migliozzi A, Palumbo R (2003) Polymer 44:369
15. Riley T, Stolnik S, Heald C et al (2001) Langmuir 17:3168
16. Hecht S, Vladimirov N, Frechet JM (2001) J Am Chem Soc 123:18
17. Hsu C-Y, Nieh M-P, Lai P-S (2012) Chem Commun 48:9343
18. Dai XH, Liu W, Huang YF, Dong CM (2011) Adv Mater Res 239: 1703
19. Dai X-H, Dong C-M, Fa H-B, Yan D, Wei Y (2006) Biomacromolecules 7:3527
20. Spain SG, Gibson MI, Cameron NR (2007) J Polym Sci A Polym Chem 45:2059
21. Kiessling LL, Gestwicki JE, Strong LE (2006) Angew Chem Int Ed 45:2348
22. Bertozzi CR, Kiessling LL (2001) Science 291:2357
23. Ladmiral V, Melia E, Haddleton DM (2004) Eur Polym J 40:431
24. Miura Y (2012) Polym J 44:679. doi:10.1038/pj.2012.4
25. Thoma G, Patton JT, Magnani JL, Ernst B, Öhrlein R, Duthaler RO (1999) J Am Chem Soc 121:5919
26. Okada M (2002) Prog Polym Sci 27:87
27. Wang Q, Dordick JS, Linhardt RJ (2002) Chem Mater 14:3232
28. Ballut S, Makky A, Loock B, Michel JP, Maillard P, Rosilio V (2009) Chem Commun 2:224
29. Laville I, Pigaglio S, Blais JC et al (2006) J Med Chem 49:2558
30. Maillard P, Loock B, Grierson D et al (2007) Photodiagn Photodyn Ther 4:261
31. Zhu G, Mallery SR, Schwendeman SP (2000) Nat Biotechnol 18:52
32. Li K, Liu B (2010) Polym Chem 1:252
33. Nederberg F, Connor EF, Möller M, Glauser T, Hedrick JL (2001) Angew Chem Int Ed 40:2712
34. Myers M, Connor EF, Glauser T, Möck A, Nyce G, Hedrick JL (2002) J Polym Sci A Polym Chem 40:844
35. Discher DE, Ahmed F (2006) Annu Rev Biomed Eng 8:323
36. Ren T, Wang A, Yuan W, Li L, Feng Y (2011) J Polym Sci A Polym Chem 49:2303
37. Li ZY, Wang HY, Li C et al (2011) J Polym Sci A Polym Chem 49: 286
38. Quimby DJ, Longo FR (1975) J Am Chem Soc 97:5111
39. Ye S, Czuba M, Romiszewska A, Karolczak J, Graczyk A (2002) Opt Appl 33:489
40. Spiller W, Kliesch H, Woehrle D, Hackbarth S, Roeder B, Schnurpfeil G (1998) J Porphyrins Phthalocyanines 2:145
41. Tada DB, Vono LL, Duarte EL et al (2007) Langmuir 23:8194
42. Gerhardt SA, Lewis JW, Zhang JZ, Bonnett R, McManus KA (2003) Photochem Photobiol Sci 2:934
43. Park SY, Han BR, Na KM, Han DK, Kim SC (2003) Macromolecules 36:411cbrs5
44. Madbouly SA, Xia Y, Kessler MR (2012) Macromolecules 45:7729. doi:10.1021/ma301458n
45. Grubbs RB (2011) Polym Rev 51:104. doi:10.1080/15583724.2011.566405
46. Siegwart DJ, Oh JK, Matyjaszewski K (2012) Prog Polym Sci 37:18. doi:10.1016/j.progpolymsci.2011.08.001
47. Gregory A, Stenzel MH (2012) Prog Polym Sci 37:38. doi:10.1016/j.progpolymsci.2011.08.004
48. Albertin L, Stenzel MH, Barner-Kowollik C, Foster LJR, Davis TP (2005) Macromolecules 38:9075
49. Bernard J, Favier A, Zhang L et al (2005) Macromolecules 38:5475
50. Dong CM, Guo YZ, Qiu KY, Gu ZW, Feng XD (2005) J Control Release 107:53
51. Ideta R, Tasaka F, Jang WD et al (2005) Nano Lett 5:2426
52. Feng H, Dong CM (2006) Biomacromolecules 7:3069. doi:10.1021/bm0605681
53. Haag R (2004) Angew Chem-Int Edit 43:278. doi:10.1002/anie.200301694
54. Moan J (1984) Photochem Photobiol 39:445
55. Choi K-H, Wang K-K, Shin EP et al (2011) J Phys Chem C 115:3212
56. Ringot C, Sol V, Barrière M et al (2011) Biomacromolecules 12:1716